Description of the p_T spectrum of the Z boson at the LHC

Mikel Mendizabal, University of the Basque Country.

Supervised by Hannes Jung and Patrick Connor

September 9, 2018

Abstract

We investigate the implementation of *Cascade* into Monte Carlo simulations (MC) to Z production in a pp collision. As *Cascade* uses already calculated TMDs from *HERAPDF*, where the kinematics of the initial state partons are known, we show that initial and final state radiations do not need to be included in the simulations.

Contents

1 Introduction

The structure of the proton is described in terms of parton distributions (PDFs). In this view, according to the scale of which is probed, the number of partons in the proton varies. At typical LHC scale, it is shown by fluctuations of gluons and pairs of $q\bar{q}$. Due to these radiations Drell-Yan (DY) can be produce (See Fig. 1) in pp collisions, where a quark and anti-quark meet and produce a Z boson.

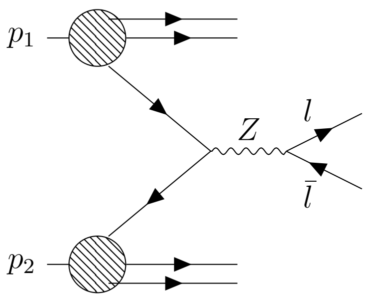

Figure 1: Decay of Z into lepton anti lepton in pp collision.

We use Monte Carlo simulations to study the p_T spectrum of the DY process. Starting with a reminder about leading and next-to leading orders, where different showers are used to test the contributions from initial and final state radiations. Then we compare leading and next-to leading order parton showers.

2 Leading Order and Next-to-leading Order

At high-energy (i.e. short-distance) interaction, QCD can be treated with perturbative theory, this property is called asymptotic freedom. However, the proton can not be treated perturbatively. The cross section in a pp collision is defined in Eq. 1 where the PDFs of each proton is needed. Fortunately, the factorisation property allows us to study the cross section with perturvative QCD and non-perturbative QCD,

$$\sigma_h = \int \underbrace{f_1 \otimes f_2}_{npQCD+pQCD} \otimes \underbrace{\hat{\sigma}_{parton}}_{pQCD}; \tag{1}$$

where σ_h is the hadronic total cross section, f_1 and f_2 the PDFs and $\hat{\sigma}_{parton}$ is the partonic cross section. The PDFs have perturbative and non-perturbative contributions: npQCD and pQCD. The pQCD here is treated with evolution equations, DGLAP (Dokshitzer–Gribov–Lipatov–Altarelli–Parisi) equations, which show us the probability of a parton to radiate. The $\hat{\sigma}_{parton}$ is also treated with perturbative QCD, in this case it is calculated using matrix-elements. The interpretation of factorisation property is a very good approach for the DY process as it is proven.

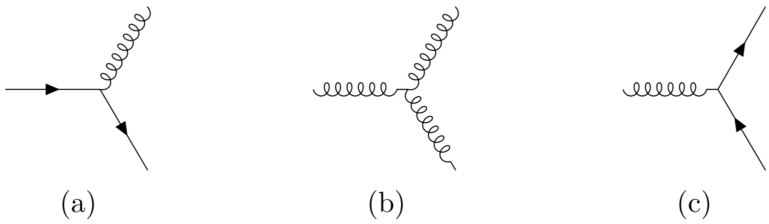

Figure 2: The three different types of parton radiation

A power expansion in α_s of the DGLAP equations (Eq. (2)) is performed for their implementation. Depending on the precision wanted in the calculations of the radiations, a higher order of the function can be achived. Starting from leading order (LO), using the first term in Eq.(2) or next-to leading order (NLO) taking the first and second terms.

$$P_{ab} = \alpha_s P_{ab}^{(0)} + \frac{\alpha_s}{2\pi} P_{ab}^{(1)} + ... \tag{2}$$

2.1 Leading order

For LO precision the first term of the expansion is used. It is important to differentiate parton shower contribution and the matrix element contribution. For the parton shower three kinds of radiations can be found: (a) gluon radiation from quark. (b) gluon radiation from gluon and (c) gluon splitting into quark anti-quark pair and (See Fig. 2). Some of these parton radiations can be seen in red in Fig. 3 an Fig. 5. At LO the hard process, the Z production, has no correction.

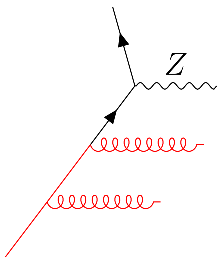

Figure 3: Leading order (LO)

The parton shower is divided into two different types: the initial state radiation (ISR) and the final state radiation (FSR). In order to see the contributions from the two types of showers, an analysis with different configurations of both showers is shown in Fig. 4 using LO showers produced with *Pythia 8*.

One directly concludes that ISR contributes the most to the MC simulations in order to fit the experimental data. However, when the extra radiation is included in the matrix elements, the ratio between data and MC increases at high values, this can happen because of contributions of hadronisations of partons in the final state, after

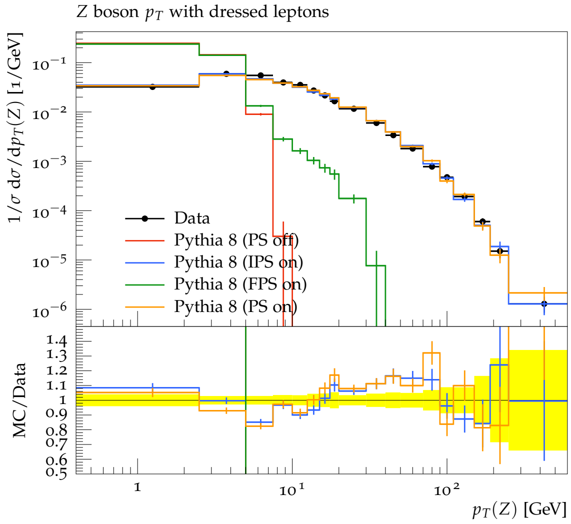

(a)

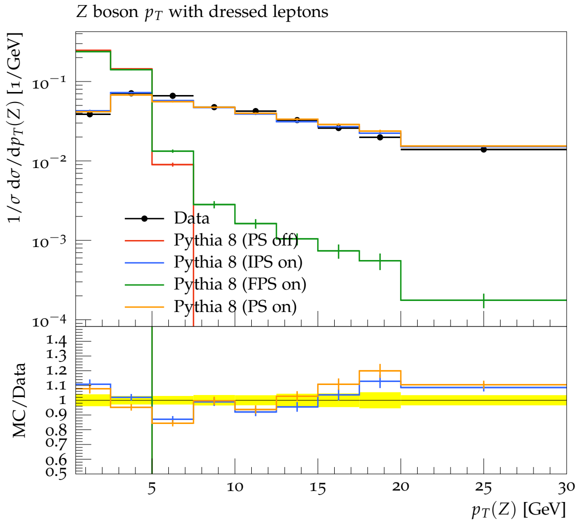

(b)

Figure 4: Normalised cross section as a function of DY p_T at $\sqrt{s} = 7$ TeV with different combinations of partons showers (PS). (a) p_T logarithmic scale. (b)p_T Linear scale. CMS analysis: [1].

every particle has the same fraction of momentum. Nevertheless, there is not much of a difference in the ratio between ISR and PS on configurations. Here the importance of the implementation of parton showers is shown.

2.2 Next-to leading order

For NLO precision from the Eq. 2 the first and second term are taken into account. At this level of precision the first corrections appear in the hard process, colored in blue in Fig. 5. In Fig. 5.a a virtual emission of a gluon is drawn. In Fig.5.b a real emission of a gluon which afterwards can split into quark anti-quark pair or radiate another gluon.

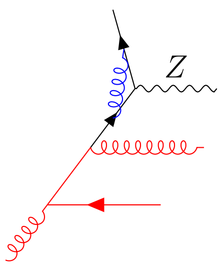

(a) Virtual emission of a gluon.

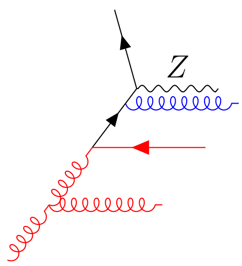

(b) Real emission of a gluon.

Figure 5: Hard process next-to leading order (NLO) in blue, parton shower correction in red.

In Fig. 6 the implementation of ISR and FSR are studied, with NLO events and parton shower. As in LO, the ISR generates most events. When FSR is included, the IFR has a noticeable shift in the high and low p_T region and overall the precision is gained with both showers considered comparing the ratios of MC and data.

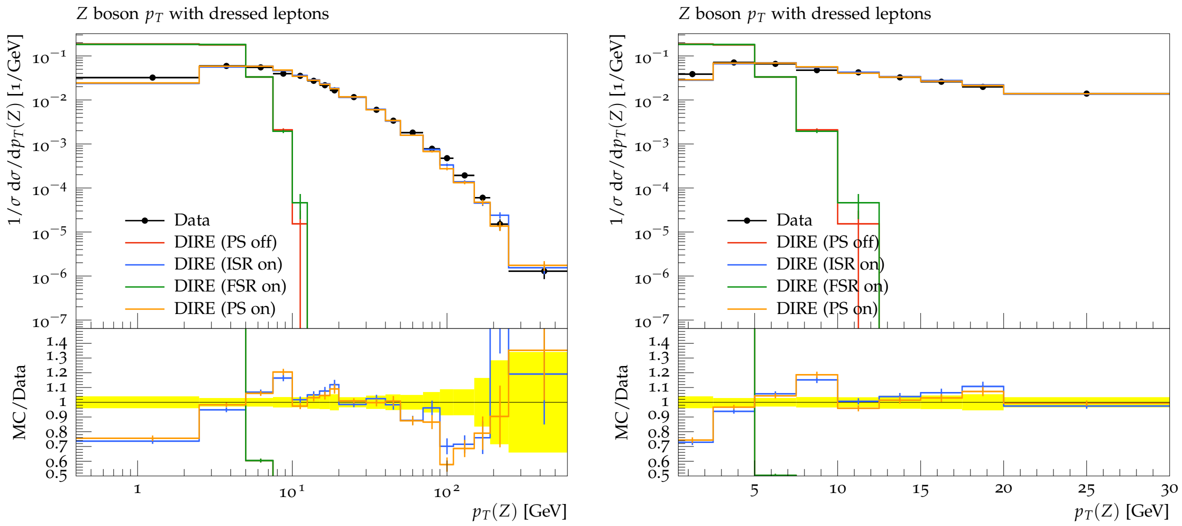

(a) (b)

Figure 6: Z production in a pp collision at $\sqrt{s} = 7$TeV, using *DIRE* shower with different configurations of ISR and FSR. (a) p_T logarithmic scale. (b)p_T Linear scale. CMS analysis:[1].

In Fig. 7 is a comparison between LO and NLO simulating a Z boson production, using *Pythia 8* for LO simulations and *DIRE* for NLO simulations. The figures show that *Pythia 8* shower is more precise than the one from *DIRE* this could be due to better tuning to CMS data. While *Pythia 8* uses CUETP8M1 tune, a CMS tune [2] to the underlying event, *DIRE* uses a default tuning, not adapted to CMS. Thus, if *DIRE* is tuned to the same level as *Pythia 8* the precision of this NLO parton shower can be expected to improve. Nevertheless, the *DIRE* showers shows a good description.

3 Phase space configuration for TMDs implementation.

For the implementation of TMDs using *Cascade*, first a configuration of the phase space. Starting for generating events using *POWHEG* and then applying some changes to the generations and afterwards using different parton showers to see the behaviour and finally we use TMDs

3.1 Event generation: POWHEG

We use *POWHEG* as a NLO event generator, producing matrix elements and first radiation, and interface it to any parton shower generator. Let $\bar{B}$ be the inclusive cross

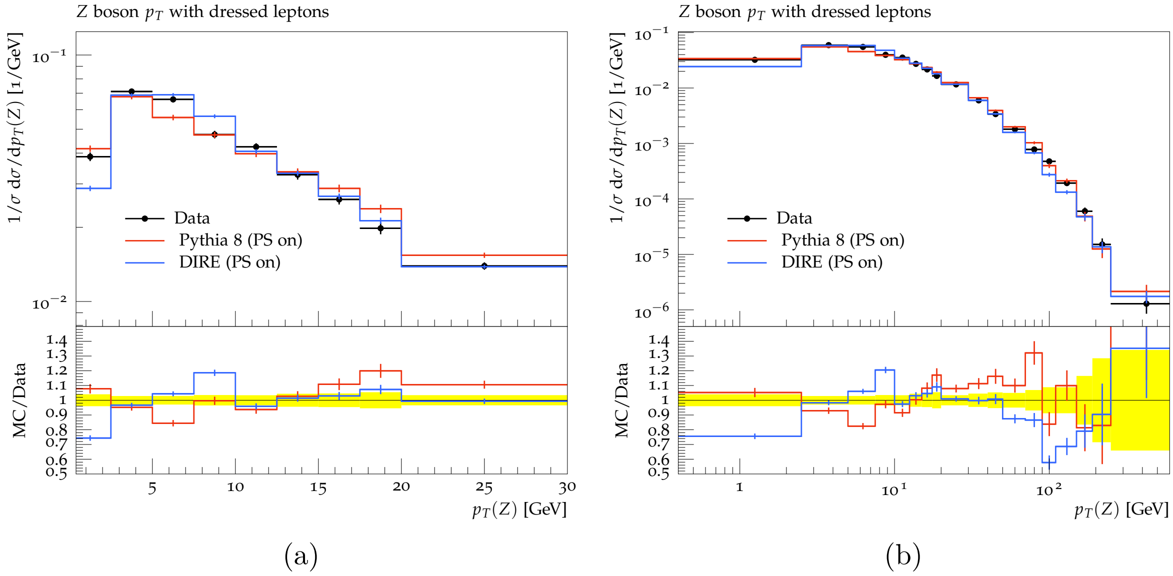

Figure 7: Normalised cross section as a function of p_T of the Z boson decaying into two leptons in a pp collision at $\sqrt{s} = 7$TeV with different combinations of partons showers using *DIRE* and *Pythia 8* showers. (a) p_T logarithmic scale. (b)p_T Linear scale. CMS analysis:[1].

section at defined Born underlying variables the corrections appear at NLO,

$$\bar{B} = B + \hat{V} + \int R d\phi_{rad}. \tag{3}$$

where B is the inclusive cross section at LO, $\hat{V}$ is the virtual emission correction and R the real cross section. R is divided into a singular part and a finite part,

$$R = R^s + R^f = \frac{h^2 m^2}{h^2 m^2 + p_t^2} R + \frac{p_T}{h^2 m^2 + p_t^2} R; \tag{4}$$

where R^s is the singular real cross section and R^f is the finite. In addition, m is the mass of the Z boson, p_T the transverse momentum and h the *hdamp* parameter. It is important to point out that this configuration in Eq.4 is only for Z production events.

The parameter h or *hdamp* has been studied. In Fig. 8 the p_T spectrum of the Z production differential cross section is shown for different *hdamp* values: 1) Default value which is infinite; 2) $h = 1$ as medium value so the term hm is of the order of the mass of the Z boson and 3) $h = 0.008$ as a small value. For the small value of *hdamp* at small and medium range the ratio of MC and data is really big and at $p_T = 2$ GeV the cross section becomes negative. For *hdamp* 1 and default the behaviour of both is almost the same with a ratio around 1 at small and medium values of p_T.

A second parameter has been used for the configuration of event generation, a $p_{T,cut}$ (the command in *POWHEG* is *ptsqmin* $= p_{T,cut}$. Whit this command *POWHEG* does not generate radiation from 0 to $p_{T,cut}$. Radiation is generated at $p_T = 0$ GeV, as in Fig. 9.a., where a cut has been implemented at 10 GeV, can be seen in the first bin. The small value of *hdamp* does not change comparing to Fig. 8, the $p_{T,cut}$ has no effect for small values of hdamp. For the other two values the cut appears at $p_T = 10$ GeV with a gap between the first bin and the cut. In consequence, $hdamp = 1$ is chosen (See Fig. 9.b.).

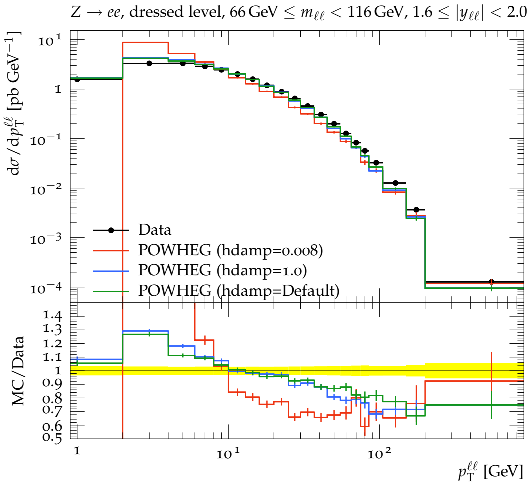

Figure 8: Z production in a *pp* collision at $\sqrt{8}$TeV, comparison for different *hdamp* values with data. ATLAS analysis: [3].

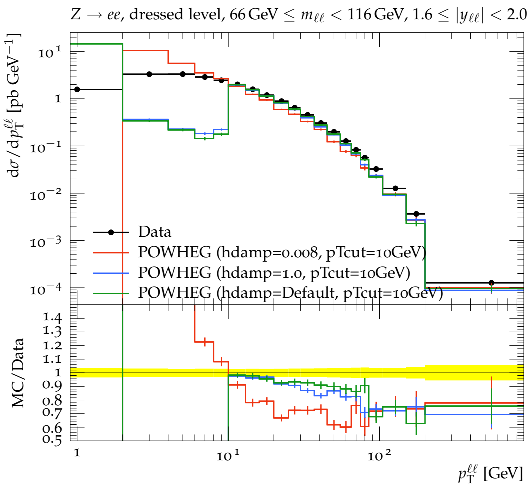

(a)

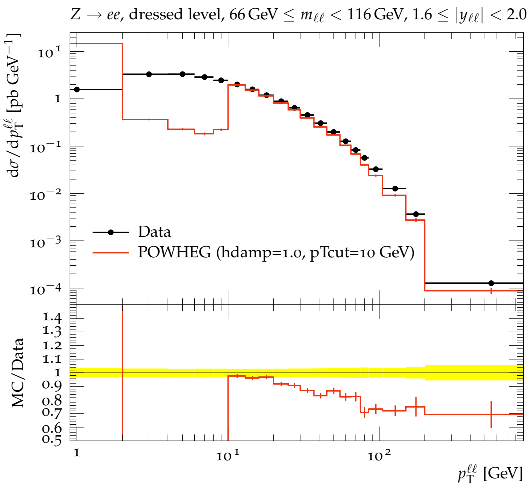

(b)

Figure 9: Z production in a *pp* collision at $\sqrt{8}$TeV, comparison for different *hdamp* values with data, $p_{T,cut} = 10$GeV. ATLAS analysis:[3].

3.2 Event showering: POWHEG + Pythia 8.

The cut is used to investigate the gap when using LO. Events generated in Fig. 9.b. are interfaced with *Pythia 8* to implement parton radiation.

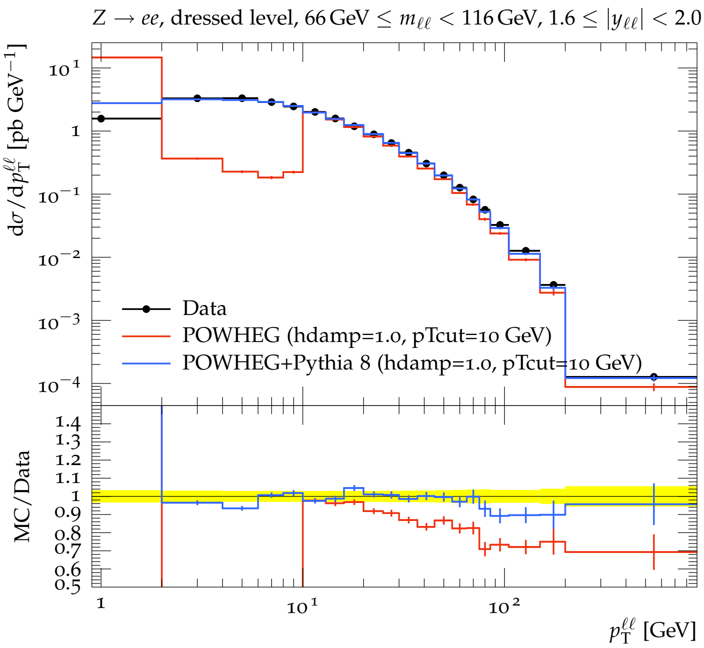

Figure 10: Merging of *Pythia 8* and *POWHEG* for Z production analysis in pp collision at $\sqrt{s} = 8$TeV. ATLAS analysis:[3].

The Fig. 10 shows the implementation of the parton shower with both ISR and FSR. The precision of the MC simulations is improved by the parton shower as a shift can be seen at medium and high p_T region. However, the displacement at low p_T from Fig. 10 and Fig. 8 taking the same *hdamp* happen because of the different Sudakov form factor for LO and NLO. In addition, the gap is very well filled by the parton shower as the ratio shows less than 10%. More information about Sudakov form factor and the NLO production can be found in [4][5].

3.3 Transverse momentum dependent PDFs (TMDs): POWHEG + Cascade.

We show the implementation of TMDs. As in the *POWHEG + Pyhtia 8* analysis, *Cascade* is interfaced replacing *Pythia 8* and substitutes the ISR by the TMDs approximation. TMDs are density functions including transverse momentum of partons. *Cascade* applies these TMDs calculated from *HERAPDF*.

Cascade applies TMDs to the initial state partons, thus, the initial kinematics of the constituents are known as well as their densities. This information allows to avoid par-

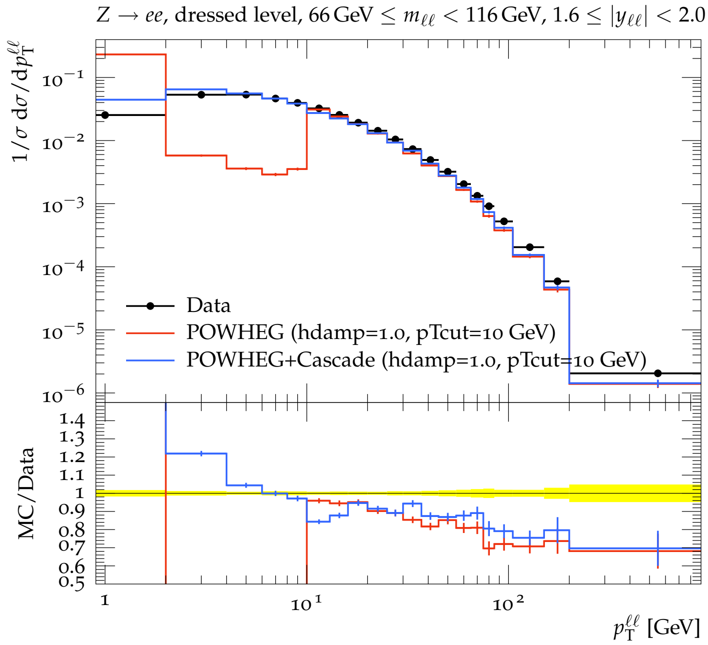

Figure 11: Merging of *Cascade* and *POWHEG* for Z production analysis in pp collision at $\sqrt{s} = 8$TeV. ATLAS analysis:[3].

ton showers to the *POWHEG* generated events. In Fig. 11 the implementation is shown: at high p_T, there shift improves the ratio of data and MC. Nevertheless, when the cut is reached from high p_T, the MC falls creating a significant step at $p_T = 10$ GeV which comes from the merging of TMDs with the real emission. Besides, the region of the gap *Cascade* is able to fill it smoothly except the low p_T region as the same happens with *Pythia 8* shower.

Fig. 12 shows how the corrections of *Pythia 8* with parton shower are more precise than the ones from *Cascade*, but this difference is not very large.

4 Conclusions

The main goal of this study, the implementation of TMDs to MC simulations, is successfully completed. The fact that the kinematics of the initial state partons are known, we are able to comprehend how partons behave when the process is happening creating a better picture of the Z production. Even though the agreement with the data of *Cascade* is not as good as *Pythia 8*, there is a huge improvement in the understanding of the DY process, as theory behind TMDs is very reliable.

When comparing LO and NLO, we have seen that the tuning of the parton shower program is of great importance to get a better agreement with the data.

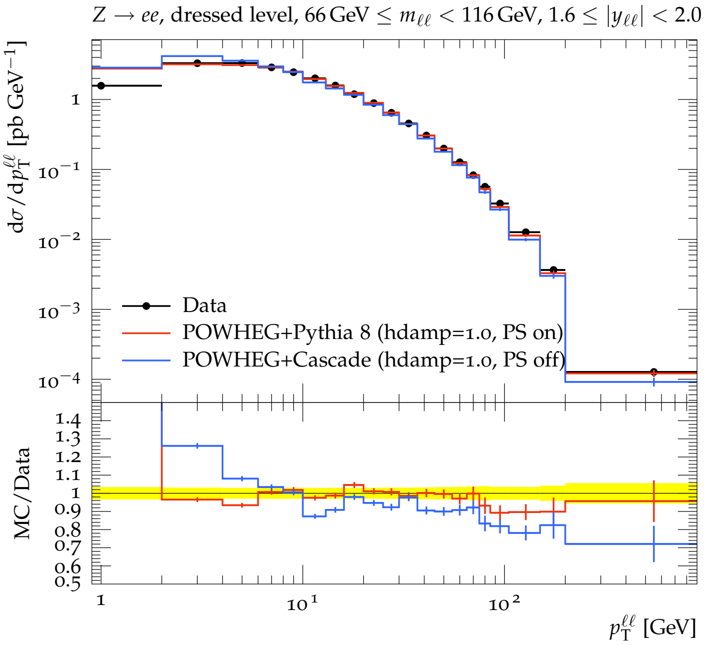

Figure 12: Comparison of *Cascade* and *Pythia 8* for Z production analysis in *pp* collision at $\sqrt{s} = 8$TeV. ATLAS analysis:[3].

Now that the first step is settled, the merging of *POWHEG* and *Cascade*, and with basic tuning works, the next step will be the improvement of the tuning as well as the merging in the cut for the step to disappear, in order to raise the ratio between data and MC.

References

[1] Serguei Chatrchyan et al. Measurement of the Rapidity and Transverse Momentum Distributions of Z Bosons in pp Collisions at $\sqrt{s} = 7$ TeV. *Phys. Rev.*, D85:032002, 2012.

[2] Vardan Khachatryan et al. Event generator tunes obtained from underlying event and multiparton scattering measurements. *Eur. Phys. J.*, C76(3):155, 2016.

[3] Georges Aad et al. Measurement of the transverse momentum and ϕ^*_η distributions of Drell–Yan lepton pairs in proton–proton collisions at $\sqrt{s} = 8$ TeV with the ATLAS detector. *Eur. Phys. J.*, C76(5):291, 2016.

[4] Stefan Höche, Frank Krauss, and Stefan Prestel. Implementing NLO DGLAP evolution in Parton Showers. *JHEP*, 10:093, 2017.

[5] Simone Alioli, Paolo Nason, Carlo Oleari, and Emanuele Re. NLO vector-boson production matched with shower in POWHEG. *JHEP*, 07:060, 2008.